

Bursting cylindrical sand balloons

Salomón Álvarez^{1,*}, Franklin Peña¹, Carlos A. Vargas¹, and Abraham Medina²

¹UAM-Azcapotzalco, Av. San Pablo 420, 02128 Azcapotzalco CDMX, México.

²ESIME Azcapotzalco, Instituto Politécnico Nacional, Av. de las Granjas 682, 02250 Azcapotzalco CDMX, México.

Abstract. We study experimentally the mechanical response of dry, cohesionless granular masses to the sudden bursts of cylindrical rubber balloons that contains Ottawa sand, at the very early instants of such an event. Due to the compression imposed by the balloon, the rupture generates a fast radial expansion of the sand front that depends on the initial radius R_0 , the initial pressure p imposed by the balloon and the effective modulus of compression, K_e . The hydrostatic compression approximation allows us the theoretical study of this problem in the context of the linear elasticity theory. We found that, at the middle part of the cylindrical balloon, *i.e.*, far from its lower and upper edges, a linear decompression wave, which induces the radial expansion of the sand front that, also, evolves linearly with time.

1 Introduction

In this study we consider a sand filled cylindrical balloon containing a mass of cohesionless grains that hangs vertically, and suddenly this mass is released by the balloon's rupture. The question is how the sand responds to the fast pressure releasing.

This phenomenon, in some sense, resembles the alighting passengers' processes, passing through the train door, in metro stations. There, it is observed that the cumulative passenger number, alighting the train displayed, an approximately linear relationship with the time [1].

In our experiments of bursting cylindrical balloons, we observed a rapid radial expansion, that at very short times, changes the volume of the granular mass but does not change its shape; such a deformation is a *hydrostatic compression* and it may be theoretical studied through the linear elasticity theory, without shear [2]. The current work is an extension of a previous study of the bursting of spherical sand balloons [3], where a decompression wave travels into the centre of the sphere and produces a radial expansion of the sand.

Understand how the granular mass behaves when the sudden bursting sand balloon occurs, it is complex. In experiments, we measured a radial expansion of the sand cylinder, mainly at its middle part, respect to the initial radius of the balloon, R_0 . However, the elasticity theory in this case predicts the existence of a decompression wave that travels into the centre of the cylinder. A correlation between both phenomena is briefly discussed.

In this study we will measure the radius R_0 of the sand filled balloon for a given mass, the absolute pressure p that the rubber balloon of radius R_0 imposes on the granular mass and the bulk density ρ of the granular material in the balloon. By knowing all these quantities and the elastic properties of a sand grain, we will estimate the effective hydrostatic compression modulus K_e , which is essential to determine the nature of the decompression wave.

During the bursting of sand balloons we will measure, using digital treatment of images, the rapid radial expansion of several masses of sand. These last measurements will be contrasted with the theoretical evolution of the elastic wave. The current study is valid during a short time, where gravity is neglected.

In order to reach our goals, this work is divided as follows. In next Section we describe the materials employed and the cylinder expansion during the bursting of sand balloons. In Section 3 we propose a theoretical analysis of the problem of the elastic decompression. Finally, in Section 4, the main conclusions and limitations of this study will be given.

2 Materials and methods

2.1 Materials

In experiments, we used specific masses, M , of Ottawa sand, composed of rounded quartz grains of average diameter 0.93×10^{-3} m, bulk density $\rho = 1670$ kg/m³, packing factor $\eta = 0.63$ and angle of repose $\theta_r = 0.58$ rad. Ottawa sand is a standard specially-graded natural silica sand with Young's modulus $E = 110 \pm 5$ GPa, density $\rho_g = 2650$ kg/m³ and Poisson's ratio $\sigma = 0.08$ [4].

* Corresponding author: vsas@azc.uam.mx

The method to measure the absolute pressure exerted by the balloon against the overall mass of sand, when the rubber balloon reaches a given radius $R = R_0$, was reported elsewhere [3]. Figure 1 shows the plot of the inflation pressure p as a function of R_0 .

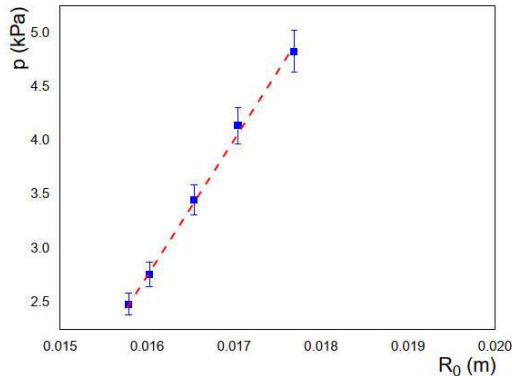


Fig. 1. Plot of the pressure p inside the balloon versus the radius of the cylindrical balloons.

2.2 Methods

Once the materials were characterized, we filled the balloons with two different masses, indicated in Table 1, where for each mass we also report the respective radius reached by the cylindrical balloon, and the inflation or compression pressure p . After the balloons were filled, they were laid to hang and then burst by exposure to an intense flame produced by a plumber's blow torch (butane/propane gas).

Table 1. Sand masses in the balloons and their corresponding mean radii, R_0 and compression pressures p . The rate of deformation gives the speed of the radial deformation of the spherical mass of grains at the earliest times of the decompression.

| Mass (kg) | R_0 (m) | p (kPa) | Rate deformation (m/s) |
|-----------|-----------------------|-----------|------------------------|
| 0.20 | 1.70×10^{-2} | 4.137 | 0.281 |
| 0.30 | 1.77×10^{-2} | 4.820 | 0.464 |

The expansion of the granular mass was experimentally visualized and measured by using high-speed photography and digital image processing, as in [3, 5]. We employed a Red Lake model HG-100K/HG-LE high-speed camera to video records the burst of each balloon at 2600 frames per second. In Fig. 2 we give a series of pics for the burst of the cylindrical balloon of mass 0.20 kg.

The deformation measurements for both masses reported in Table 1 (defined as $deformation = r(t) - R_0$) are given in Fig. 3 and were obtained with a very accurate image treatment [6]. They correspond to the radial deformation when the granular material is even so packed to allow measure the continuous sand front, through an average of several measurements in vertical positions close to the red line. The sand deformations have flat parts (delays) and after they evolve linearly with time. The rate deformation in Table 1, corresponds to the time derivative of the deformation of the straight

lines in Fig.3. For times longer than $t=0.012$ s, in Fig. 4, we give pics where the radial motion of the grains is visible, Figs. 4(a)-(b). In Fig.4(c) we show the instantaneous thickness of the front obtained from the subtraction of pictures 4(b) and 4(a), with temporal separation $\Delta t=0.0004$ s.

Finally, we must notice that for times slightly longer than $t=0.012$ s, gravity dominates and it causes the grains to spill, and then the model fails to be valid.

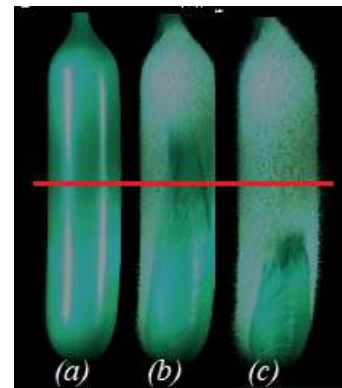


Fig. 2. Pics of the sand filled cylindrical balloons; (a) previous to the rupture, (b) $\Delta t=16 \times 10^{-4}$ s after the rupture and (c) $\Delta t=28 \times 10^{-4}$ s after the rupture.

In the next Section we will propose a theoretical model to explain the decompression of the granular material, founded on the linear elasticity theory [2].

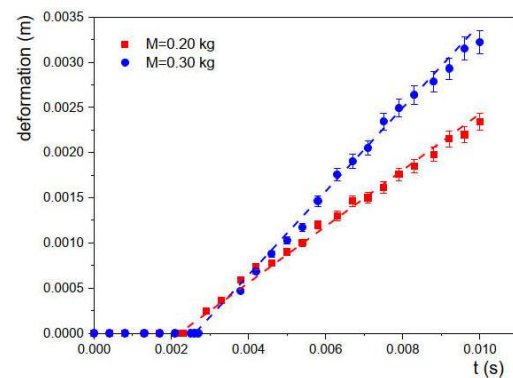


Fig. 3. Plot of the radial deformation of the sand cylinders of different masses, as a function of time, due to the sudden decompression of the granular masses. Error bars are of 4%.

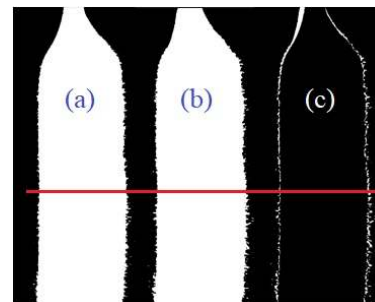


Fig. 4. (a) and (b), pics of the deformation of the sand cylinder after $t=0.012$ s. (c) shows the axisymmetric expansion obtained from the subtraction of pics (a) and (b).

3 Theoretical analysis

3.1 Linear elasticity model

Our theoretical treatment of the elastic response of the granular mass as an effective medium, to the sudden release of the radial pressure, is essentially valid far from the upper and lower edges of the cylinder, *i.e.*, at the middle part of it, because there the material was subjected to a uniform radial compression p , and its deformation is purely radial, as can be inferred from the radial expansion observed in the previous experiments.

In order to obtain the equation of motion for the elastic medium, we must equate the internal stress force $\partial\sigma_{ik}/\partial x_k$ to the product of the acceleration $\partial^2\mathbf{u}/\partial t^2$ and the bulk density ρ . The quantity $\mathbf{u}(\mathbf{x},t)$ is the displacement vector of the effective medium subsequent to the suppression of the rubber film, the variation of the stress tensor relative to that of the compressed medium is $\sigma_{ij} = K_e \nabla \cdot \mathbf{u} \delta_{ij}$, where K_e is the effective compressibility modulus, $\nabla \cdot \mathbf{u}$ is the trace of the strain tensor, and δ_{ij} is the identity tensor [2]. With cylindrical symmetry, leaving out the effect of gravity in the early stages of the expansion, we have $\mathbf{u} = u(r)\mathbf{e}_r$, where r is the distance from the balloon center and \mathbf{e}_r is a unit vector in the local radial direction. Then $\nabla \cdot \mathbf{u} = 1/r(\partial(ru)/\partial r)$, and the deformation under hydrostatic compression satisfies the wave equation

$$\rho \frac{\partial^2 u}{\partial t^2} = K_e \frac{\partial}{\partial r} \left[\frac{1}{r} \frac{\partial(ru)}{\partial r} \right]. \quad (1)$$

An order-of-magnitude estimation of the time for which the decompression occurs in a fast manner (in the absence of gravity) is obtained through Eq. (1). If the inertial force is of the same order than the hydrostatic compression when the granular mass has a size $r = R_0$, then $\rho u/t^2 \sim K_e u/R_0^2$, meaning that $t \sim \sqrt{\rho R_0^2/K_e}$. Therefore, our theoretical analysis is valid for times that fulfill such a condition.

Equation (1) must be solved subject to the boundary conditions

$$r = 0: u = 0 \text{ and } r = R_0: \sigma_{rr} = pH(t), \quad (2)$$

where H is the Heaviside step function, defined as $H(t)=0$ if $t < 0$ and $H(t)=1$ if $t \geq 0$.

These consist of the symmetry condition at the center of the balloon and the condition that the pressure of the rubber film is instantly released at $t=0$. The initial conditions are

$$t \rightarrow -\infty: u = \frac{\partial u}{\partial t} = 0. \quad (3)$$

The solution of the Eq. (1) subject to the conditions (2) and (3) is

$$u(r, t) = \frac{p}{2K_e} [ct + (r - R_0)]H\left(t + \frac{r-R_0}{c}\right), \quad (4)$$

which represents a wave moving towards the center of the balloon at a constant speed $c = \sqrt{K_e/\rho}$. Clearly, this solution depends on the effective modulus of hydrostatic compression K_e , which, for a random packing of spherical grains that interacts without shear stresses, has the form [3]

$$K_e = \frac{3}{2^4\pi^{2/3}} (\eta N_c)^{2/3} \left(\frac{E}{1-\sigma^2}\right)^{2/3} p^{1/3}, \quad (5)$$

here N_c is the mean number of neighboring spheres $N_c=6$ [3, 8]. The values of the elastic grain's parameters were given in Subsection 2.1.

3.2 Plots of the waves

By using the materials' data and the experimental realizations, given in Section 2, we have performed a series of plots that describe the wave motion in each balloon, Eq. (4). The plots of $u(r,t)$ show the evolution of the decompression wave at a fixed position r , within the granular mass, or at a given time t , after the start-up of the decompression motion.

To reach this goal, we first need estimates the value of the effective modulus of hydrostatic compression K_e , through Eq. (5), which depends strongly on the compression pressure p imposed by the balloon. In Table 2 we give the vale of K_e and the speed of the wave $c = \sqrt{K_e/\rho}$, for each cylindrical balloon reported in experiments.

Table 2. Values of K_e and c of each bursted balloon experiment.

| $R_0(m)$ | $K_e(kPa)$ | $p(kPa)$ | $c (m/s)$ |
|-----------------------|--------------------|----------|-----------|
| 1.70×10^{-2} | 7.85×10^4 | 4.13 | 216.82 |
| 1.77×10^{-2} | 8.26×10^4 | 4.82 | 222.41 |

In Fig. 5 we give the plots of $u(r,t)$ vs t which were computed with Eq. (4) and data of Table 2, for the radial position $r = 0.015$ m, within the granular mass. The dashed red line corresponds to the decompression wave moving towards the center of the small balloon of radius $R_0=0.0170$ m and the blue one corresponds to big balloon, of radius $R_0=0.0177$ m.

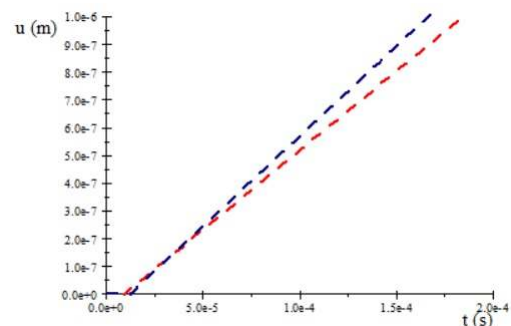


Fig. 5. Plots of the decompression wave u at $r = 0.015$ m (Eq. (4)). Dashed red line corresponds to the cylindrical balloon of radius $R_0=0.0170$ m and the blue one to radius $R_0=0.0177$ m.

In Fig. 6 we give the plots of $u(r,t)$ vs r , which were computed in the same manner as those in Fig. 5, but now for the fixed time $t=4 \times 10^{-5}$ s. The dashed red line corresponds to the decompression wave moving towards the center of the balloon, of radius $R_0=0.0170$ m, and the blue one corresponds to the wave in the balloon of radius $R_0=0.0177$ m.

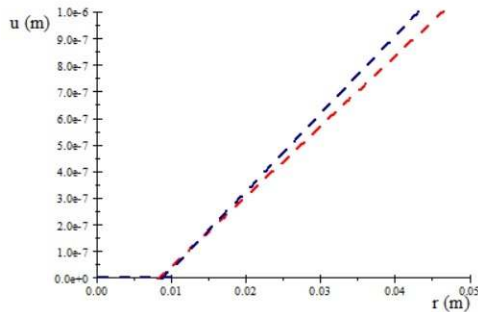


Fig. 6. Plots of the decompression wave $u(r,t)$ for $t = 4 \times 10^{-5}$ s (Eq. (4)). Dashed red line corresponds to the cylindrical balloon of radius $R_0=0.0170$ m and the blue one to radius $R_0=0.0177$ m.

By looking at Fig. 5, we see that the decompression waves in the cylindrical balloons have a delay, and a short time after a linear displacement, with speed $c=216.82$ m/s for the balloon of radius $R_0=0.0170$ m, and with $c=222.41$ m/s for the bigger balloon, as is reported in Table 2. Also, in Fig. 5 it is noticed that when the motion starts, the temporal displacement in the small cylinder is slightly larger than in the big one, but, after a short time, the opposite occurs.

A similar behavior has been observed in the *deformation* given in plots of Fig. 3. Consequently, we can infer that the decompression wave produces an expansion of the granular mass but with a slower motion than that predicted for the decompression waves. This behavior is different than that occurring in dilatancy [9], where the volume change observed in granular materials occurs when they are subjected to shear deformations.

Finally, we observe that the small elastic radial displacements given in plots of Figs. 5 and 6 occur at very short times in comparison with the radial volumetric expansion of the granular mass reported in Fig. 3.

4 Conclusions

In this work, experiments show the occurrence of a radial expansion (*deformation*) that first has a delay and after obeys a linear evolution, as a function of time (Fig. 3). Through the linear elasticity theory, specifically using the hydrostatic compression approximation [2], we have obtained that the elastic displacement $u(r,t)$ is a decompression wave which, at a fixed distance r , travels towards the center of the cylindrical mass with a delay in the time and, after, a linear evolution with time.

In Section 3, we found that the decompression wave in the cylindrical mass is fast, because it travels at a speed of $c = \sqrt{K_e/\rho} \sim 200$ m/s. Alluding to the previous results, we remark that when an elastic wave passes through the dense granular medium, particles within that medium don't travel with the wave; instead, they oscillate around their equilibrium positions which are characterized by Eq. (4). The actual axisymmetric deformation, reported in Fig. 3, corresponds to the reactive motion of the edge of the granular cylinder (measure in a small region close to the red line in Fig. 2) as a time function, and we understand it as a response of the noncohesive grains to the wave's penetration into the core of the cylinder. In agreement with it, the simple optical visualization does not allow the detection of the inner motion of the elastic wave. Due to all these limitations, more experimental studies to connect the deformation measurements of the sand cylinder with the elastic waves, are now undertaken.

Authors acknowledge to Y. Hernández, G. Gómez from IPN and to F.J. Higuera from Universidad Politécnica de Madrid, their aid in several stages of the elaboration of this work.

References

1. Y. Qu, Y. Xiao, H. Liu, H. Yin, J. Wu, Q. Qu, D. Li and T. Tang, Analyzing crowd dynamic characteristics of boarding and alighting process in urban metro stations, *Physica A* **526**, 121075, (2019)
2. L.D. Landau and E.M. Lifshitz, *Theory of Elasticity* (Elsevier: Oxford, UK, 2015)
3. G. Gómez, F.J. Higuera, F. Sánchez-Silva and A. Medina, Bursting sand balloons. *Fluids* **9**, 49, (2024)
4. S.T. Erdogan, A.M. Forster, P.E. Stutzman, and E.J. Garboczi, Particle-based characterization of Ottawa sand: Shape, size, mineralogy, and elastic moduli. *Cem. Concr.* **83**, 36, (2017)
5. W. Cao, H. Liu, W. Li and J. Xu, The characteristics of the near field of the granular jet. *Fuel* **115**, 17, (2014)
6. Y. Hernández, *Descompresión súbita de una masa granular* Master Thesis, ESIME'UA, IPN, México, 2023
7. J.P. de Bono and G.R. McDowell, An insight into the yielding and normal compression of sand with irregularly-shaped particles using DEM. *Powder Tech.* **271**, 270, (2015)
8. K. Walton, The effective elastic moduli of a random packing of spheres. *J. Mech. Phys. Solids* **35**, 213, (1987)
9. O. Reynolds, Osborne. "LVII. On the dilatancy of media composed of rigid particles in contact. With experimental illustrations". *The London, Edinburgh, and Dublin Philosophical Magazine and Journal of Science.* **20** (127), 469, (1885)